

The Research and Application of the MEMS-IMU in the Maglev Train

PENG, Zengde^{1, a}, Dou, Fengshan^{2, b}, Long, Zhiqiang^{3, c}

¹ College of Intelligence science, National University of Defense Technology, Changsha, Hunan, 410073.China

² College of Intelligence science, National University of Defense Technology, Changsha, Hunan, 410073.China

³ College of Intelligence science, National University of Defense Technology, Changsha, Hunan, 410073.China

^apengzengde16@126.com, ^bdfs5460@126.com, ^clzq@maglev.cn

Key word: MEMS technology, Random walk, sailing gesture, wavelet transform, Multi-information Fusion

Abstract. This paper focuses on the optimal design for the immunity and accuracy of the Speed measurement and location in the maglev train. First, based on the analysis of the error model of the MEMS-IMU, an algorithm which based on Mallat wavelet transform and absolute state recognition for cumulative error correction is applied to effectively compensate and correct the error of MEMS inertial sensor. Then, an optimization algorithm of fusion speed measurement and location is proposed to improve the stability and speed accuracy of the speed measurement and location system.

Introduction

In view of the separation of medium and low-speed maglev train from rail, it's necessary to provide speed signals for train and signal system through non-contact speed measurement. Existing non-contact speed measurement and location techniques principally include German high-speed maglev TR series relative speed measurement and location and absolute location techniques [1], as well as medium and low -speed maglev speed measurement with sleepers sensed with inductive sensor [2], cross-inductive looped-cable speed measurement technique [3], and radar speed measurement technique etc. All difficult points of above-noted speed measuring techniques lie in how to effectively improve speed measurement accuracy and speed signal stability; Literatures [1, 3-8] improve the speed measuring & location accuracy and stability through multi-sensor information fusion and fusion optimized algorithms. The schematic diagram of the scheme for speed measurement & location with sleepers sensed by inductive sensor [2] (hereinafter referred to as SMD-IASS) is roughly shown in Fig. 1. The mean speed is determined based on the time difference between adjacent sensors A1 and A2 passing through the same sleeper, as well as the distance between the said two sensors [2]. This scheme features simple structure, low cost, and high system reliability, but it brings about problems such as the significant system error in low-speed operation of train and the limited resistance to fluctuation-induced stochastic error of train levitation system. On this basis, the present paper deals with the way to improve medium and low-speed maglev train speed measurement & location accuracy and stability etc. through the study on the adoption of MEMS-IMU in medium and low-speed maglev train speed measurement & location system. Despite the obvious superiority of MEMS-IMU, it's still important to eliminate the cumulative error and drift in MEMS-IMU. Due to the limitations of MEMS inertial sensor's operating principle and internal manufacturing process, MEMS-IMU output signal exhibits shortcomings such as drift, non-stationarity and slow time variation [10,11]. Literatures [5-11,15-16] performed modeling analysis and filtering operation for MEMS error model. Error modeling methods principally include time series analysis method, neural network, and wavelet analysis method etc., while the filtering methods include Kalman filtering, robust filtering, non-linear filtering and their optimized filtering algorithms etc. [11]. Analysis showed that it's extremely difficult for linear filter to filter the noise effectively; in contrast, wavelet transform enables translation and stretching

transformation using Wavelet Basis function that features fast convergence and local concentration of energy, thereby analyzing the characteristics of signals in time domain and frequency domain; moreover, it's possible to analyze and denoise signals based on multiple resolutions analysis [13-16].

To this end, this paper denoises MEMS-IMU signal using wavelet transform filtering algorithm, determines the acceleration in travel direction through attitude computation of the signal measured by MEMS-IMU, and fuses the acceleration computed through MEMS-IMU and the speed and acceleration obtained based on SMD-IASS system, thereby improving the accuracy and stability of speed measurement.

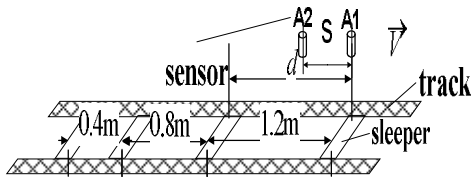


Fig. 1 Schematic diagram of sleeper sensed measurement by inductive sensor

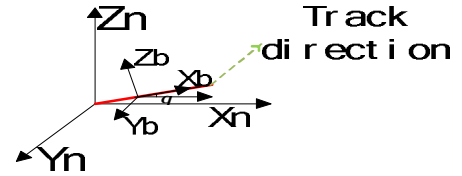


Fig. 2 Schematic diagram of simplified model of motion attitude

Mathematical Analysis of MEMS-IMU Based Fusion Speed Measurement Algorithm

The effect of navigation angle on the acceleration and angular speed in climbing direction is substantially negligible due to the fact that the max. climbing angle of existing medium and low-speed maglev tracks is approx. 4° , and that their min. turning radius is approx. 50m. Hence, the travel attitude of magnetically suspended train can be simplified into angle q between track direction (i.e. carrier coordinate system X_b) and navigation coordinate system (z coordinate system) on X axis, as shown in Fig. 2.

Assuming the inherent noise interference of MEMS acceleration and angular speed is xa and xw respectively, and that the vehicle vibration-induced noise interference is xa_1 and xw_1 respectively, the mathematical relationship between MEMS-IMU measured value and true value should be Eq. 1. (d) and (e) in Eq. 1 summarize the error model of main interference to MEMS-IMU. Where, a_{car_x} represents train traction/braking-induced acceleration; Xa is the simplified error model of x -axis accelerometer; XW means the simplified error model of z -axis gyroscope; composed of first-order Markov process drift (S_{wz} is scale factor error), zero offset B_{wz} and Gaussian white noise n_{wz} , the Xa error type is similar to that of XW .

The speed measurement & location model incorporating SMD-IASS system and MEMS-IMU based on kinematic theory is shown in Eq. 2. Where, \bar{v}_{ls} represents the speed determined through SMD-IASS system; Δt is the vehicle acceleration integrating period between adjacent sensors; a_{car} stands for vehicle acceleration; a is the real time difference of the adjacent sensor through the same sleeper. The speed determined through MEMS-IMU system is $\Delta v = \int a_{car} dt$; the speed $\bar{v}_{ls} = \bar{v}_{ls} + \Delta v$ is updated in real time between adjacent inductive sensors. This helps to improve speed and location accuracy.

$$\begin{cases}
 \dot{W}_{MEMS_x} = W_{gui_x} + \dot{x}W + \dot{x}W_1 & (a) \\
 \dot{q} = q_{gui_x} + \int (\dot{x}W + \dot{x}W_1) dt & (b) \\
 a_{MEMS_x} = a_{car_x} - g \sin q + \dot{x}a + \dot{x}a_1 & (c) \\
 \dot{x}a = (1 + S_{ax})a_{car_x} + B_{ax} + n_{ax} & (d) \\
 \dot{x}W = (1 + S_{wx}) \times W_I + B_{wx} + n_{wx} & (e)
 \end{cases} \quad (1)$$

$$\begin{cases}
 \bar{v}_{1s} = \frac{s}{\Delta t_1} & (a) \\
 v_{0s} = v_{1s} & (b) \\
 v_{1s} = \bar{v}_{1s} + a_{car} \times \Delta t & (c) \\
 a_s = \frac{v_{1s} - v_{0s}}{\Delta t_1} & (c) \\
 S_{1s} = S_{0s} + v_{1s} \times \Delta t + \frac{a_{car} \times \Delta t}{2} & (e) \\
 \Delta t_1 = \Delta t_1^- + x_{1t} & (f)
 \end{cases} \quad (2)$$

Considering the interference of the inductive sensor, the time differences Δt_1 of detecting the same sleeper by the adjacent sensor has significant stochastic errors x_{1t} , which may impair the speed measurement accuracy and stability. Hence, speed jump resulting from random disturbance on inductive sensor should be prevented by fusing MEMS-IMU acceleration and \bar{v}_{1s} . In view of the obvious cumulative error of long-time integration for MEMS-IMU angular speed, MEMS-IMU should be denoised; furthermore, in consideration of the fact that all angle and position values attained based on SMD-IASS and MEMS-IMU speed measurement & location systems are relative values, cumulative error must be compensated for by developing a cumulative error correction algorithm for absolute state recognition.

Mallat Wavelet Transform Optimization Algorithm Based Analysis

Mallat Wavelet Transform

To address the orthogonality and computation load between wavelet transform, this paper employs mature wavelet transform algorithm, i.e. pyramidal multi-resolution analysis and restructuring fast algorithm (Mallat algorithm[12]), and analyzes the optimization of its derivation process and data boundary[17].

Assuming $f(t) \in L^2(R)$, that the space $A_j f \in V_j$ of $f(t)$ at resolution 2^{-j} has been obtained, and that $\{V_j\}_{j \in \mathbb{Z}}$ constitutes the multi-resolution analysis of $L^2(R)$, then $V_j = V_{j+1} \oplus W_{j+1}$, namely:

$$A_j f = A_{j+1} f + D_{j+1} f \quad (3) \quad \begin{cases} A_j f = \sum_{k=-\infty}^{\infty} a_{j,k} j_{j,k}(t) \\ D_j f = \sum_{k=-\infty}^{\infty} d_{j,k} y_{j,k}(t) \end{cases} \quad (4)$$

Where, $y_{j,k}(t)$ represents wavelet function, and $j_{j,k}(t)$ is wavelet scale function.

$$a_{j,k} = \langle f, j_{j,k} \rangle, d_{j,k} = \langle f, y_{j,k} \rangle.$$

According to two-scale equation:

$$\begin{cases} j_{j,k}(t) = \sum_{m=-\infty}^{\infty} h(k-2m) j_{j,m}(t) \\ y_{j,k}(t) = \sum_{m=-\infty}^{\infty} g(k-2m) y_{j,m}(t) \end{cases} \quad (5)$$

Where, $h(k-2m) = \langle j_{j,m}, j_{j,k} \rangle$, $g(k-2m) = \langle y_{j,m}, y_{j,k} \rangle$. The relations above lead to:

$$\left\{ \begin{array}{l} a_{j+1,m} = \sum_{k=-\infty}^{\infty} h_{(k-2m)} a_{j,k} \\ d_{j+1,m} = \sum_{k=-\infty}^{\infty} g_{(k-2m)} a_{j,k} \end{array} \right. \quad (6) \quad a_{j,k} = \sum_{k=-\infty}^{\infty} h(k-2m) a_{j+1,m} + \sum_{k=-\infty}^{\infty} g(k-2m) d_{j+1,m} \quad (7)$$

Eq. 6 is Mallat one-dimensional decomposition function, and Eq. 7 is Mallat one-dimensional restructuring function. Since the limited length of signal may bring about boundary discontinuity in practical application of Mallat algorithm, cycle extension method helps to alleviate slow transformation coefficient attenuation at boundary to a certain extent; cycle extension method is realized by reducing Eq. 6 to Eq. 8 and putting the first two values of the sequence at the end to create a circular sequence.

$$z(k) = \sum_{l=0}^{l_{\max}} f(l)x(l+2k) \quad (k \in Z) \quad (8)$$

Where, the scale expansion coefficient $z(k)$; the coefficient is $f(l)$ (conjugate filter coefficient); $x(l+2k)$ is the input sequence after signal discretization; l_{\max} is the maximum value of data sequence, and the maximum is $\frac{N}{2} - 1$.

Wavelet Restructuring Function Optimization Algorithm

Due to the favorable regularity of medium-to-low speed maglev track, track curvature variation-induced angular speed frequency is lower than 2Hz. Hence, the approximation signal component of max. decomposition scale can be used as restructuring signal. Due to the full-band distribution of MEMS-IMU noise, however, colored noise still exists in approximation signal. According to analysis result, the detail wavelet coefficient is low at the max. scale of MEMS-IMU noise, so the coefficient values below W (the max. coefficient value determined based on statistics made in static suspension state) can be set to zero; in consideration of the fact that angular speed changes symmetrically in climbing stage, the signal loss has no effect on the angle value obtained through integration. Assuming the max. decomposition layer count to be N , and the max. decomposition scale to be 2^N , then:

$$h(k-2N) = \begin{cases} h(k-2N), & h(k-2N) > W \\ 0, & h(k-2N) < W \end{cases} \quad k = -\infty \sim +\infty.$$

When h is obtained through calculation based on Eq. 6, 7 and Eq. 9, the restructuring signal is expressed as:

$$A_0 f = V_0 = h a_{N,k} \quad (9)$$

Cumulative Error Correction Algorithm for Absolute State Recognition

Angle and vehicle acceleration should be subjected to cumulative error correction in order to further improve speed measurement & location accuracy. According to the basics of circular curvature, train climbing angle changes slowly; it is observed from Eq. 10 that track slope change rate brings about low acceleration change rate. The order of magnitude of maglev train acceleration/deceleration, however, is apparently higher than track slope-induced variation at the start time of traction/braking operation. Based on this characteristic, it's possible to identify the state of train, i.e. free sliding or traction/braking.

$$a = g * \sin q \Rightarrow \lim_{x \rightarrow 0} (\Delta a = g \sin(\Delta q)) \Rightarrow \lim_{x \rightarrow 0} (\Delta a = g \Delta q). \quad (10)$$

The reliability of zero speed and constant speed identification is improved through the fusion of multi-sensor signals, the identification formulas are shown in Eqs. 11 and 12 respectively. The train stop state characteristic is obtained By detecting the number of sensor signal flips(N) in time Δt_0 ; Moreover, sliding window is used to observe the acceleration variance $d_{a_I}^2$ in order to effectively detect the sudden change of acceleration, and Combined with the speed difference to determine the constant speed state characteristic of train; then, it is updated and corrected using Eq. 13. Fig. 3 shows the improved fusion speed measurement and location system.

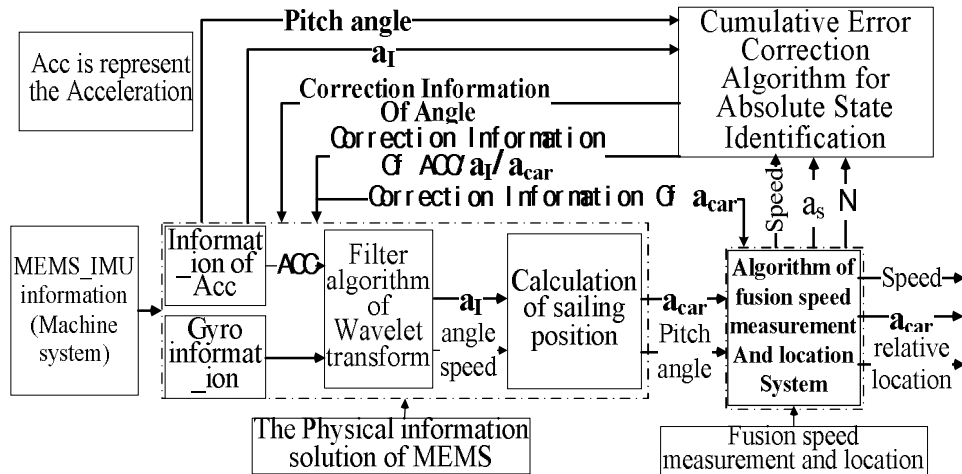


Fig. 3 Wavelet based optimized fusion speed measurement & location system

$$\lim_{\Delta t \rightarrow \Delta t_0} \sum_{N=0}^{\infty}$$

(11)

$$\begin{cases} a_s < z A1 \\ d_{a_I}^2 = \frac{1}{n} \sum_{j=k}^{j=k+n} (a_I - E(a_I))^2 < z A2 \\ \lim_{t \rightarrow t_0} \Delta v < z A3 \end{cases} \quad (12)$$

$$\bar{a}_I = \frac{1}{n} \sum_{j=k}^{j=k+n} a_I \cdot q_{\text{Check}} = \sinh(\bar{a}_I / g) \quad (13)$$

Where, N represents the number of inductive sensor signal turnovers; Δt_0 is the stop state identification time determined through SMD-IASS statistics; a_s means the acceleration obtained through SMD-IASS; $z A1$ stands for the statistic for confirming the train to be in constant speed characteristic obtained through SMD-IASS statistics. $d_{a_I}^2$ represents acceleration variance, $z A2$ is its confidence interval statistic; Δv is the speed difference, $z A3$ is a statistic that the train is judged to be in a constant speed characteristic according to the speed difference within time t_0 ; a_I is the acceleration after wavelet transform of MEMS-IMU; \bar{a}_I represents the mean value of a_I .

Wavelet Based Fusion Speed Measurement and Location Experiment Verification

This study is based on the MEMS-IMU system. The original signal measured by the accelerometer is tremendous noisy, while the original signal measured by the gyroscope is submerged by noise, as shown in Figs. 4 and 5 respectively. The test is performed using Mallat one-dimensional algorithm; since the curve of angular speed in time domain is similar to that of db4, db4 is chosen as the wavelet base for wavelet transform [16]. Since the max. track slope is 7%, the cycle of train operation with slope is more than 5s according to the prior knowledge about low-speed maglev transportation

operation, which is to say, the frequency is lower than 0.2Hz. In consideration of engineering error, the maximum frequency of the acceleration signal caused by the change of track slope is assumed to be 0.4 Hz. Because MEMS_IMU acquires data at a rate of 819.2Hz, 12-layer wavelet decomposition is available. The test result is analyzed below.

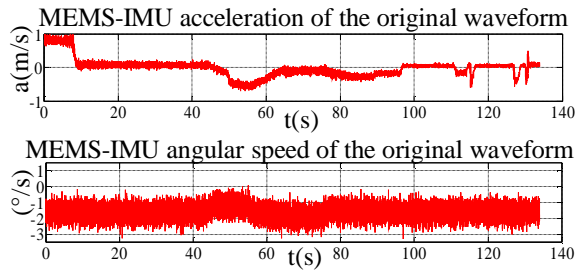


Fig. 4 Original waveforms of MEMS-IMU

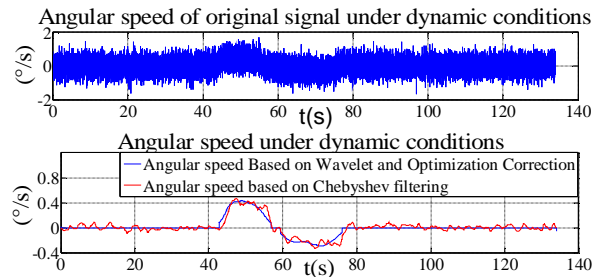


Fig. 5 Comparison diagram of angular speed in dynamic moving state

This is a dynamic running test, where MEMS-IMU and SMD-IASS data is acquired in real time during the travel of train. Started from stationary state, the maglev train climbed a 4-degree slope and stopped after running for 134s, having traveled a distance of 692m. Refer to Figs. 5, 6, 7, 8 and 9 for the angle, acceleration, speed, and relative location parameters determined by processing the test data through wavelet transform, optimized fusion algorithm for speed measurement, and cumulative error correction algorithm.

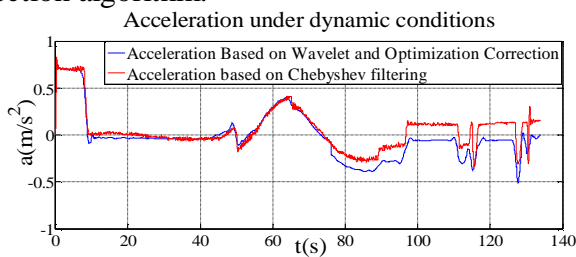


Fig. 6 Comparison diagram of vehicle acceleration in dynamic moving state

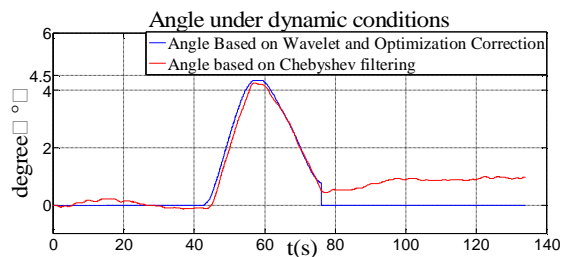


Fig. 7 Comparison diagram of angle in dynamic moving state

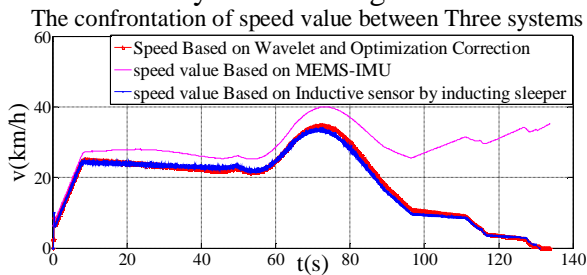


Fig. 8 Comparison diagram of speed in dynamic moving state

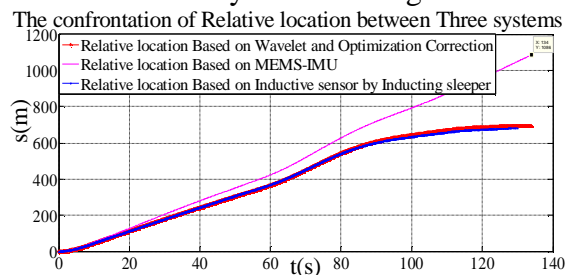


Fig. 9 Comparison diagram of relative location in dynamic moving state

Due to the existence of zero offset and random walk in MEMS, the long-time integral of angular speed leads to a large cumulative error in angle, and the acceleration deviation increases due to the attitude solution, which causes the speed to diverge. As shown in Figs. 7, 8 and 9, the angle, speed and relative location exhibit significant divergence if wavelet transform and speed optimized fusion algorithm are not used for data processing. The data acquired after the initial 10s is substantially useless. Table 1 shows the detailed comparison between the three speed measurement & location systems in terms of relative location accuracy.

Table 1 Statistical table of mileage errors of the three systems for relative location.

Total mileage: 692m	Mileage (m)	Error (m)
Wavelet + fusion system	693.2	1.2
MEMS-IMU system	1086	394
SMD-IASS system	679.2	12.8

To verify the stability of wavelet transform and fusion information based speed measurement & location system, random interference components $\pm 0.5 \text{ m/s}^2$ and $\pm 15 \text{ km/h}$ are respectively added to the acceleration and speed values calculated by SMD-IASS as shown in Fig. 10. Fig. 11 shows the speed parameter obtained by means of wavelet transform and fusion speed measurement optimization algorithm; the max. error of speed is 2 km/h, which indicates the remarkable improvement in stability of speed measurement system.

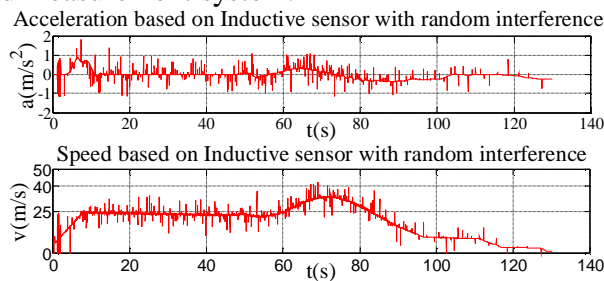


Fig. 10 Random interference of SMD-IASS acceleration and speed

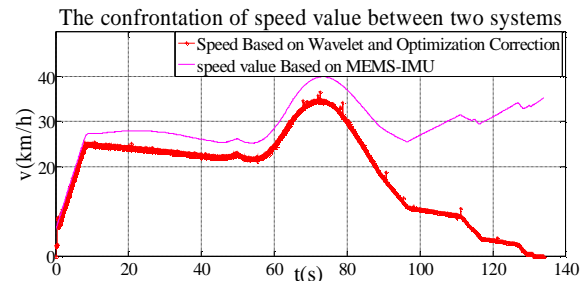


Fig. 11 Speed comparison diagram with random disturbance

Conclusion

This paper employs wavelet transform filtering algorithm, fusion speed measurement algorithm and cumulative error correction algorithm for absolute state recognition to have overcome the effect of weak non-linearity, non-stationarity, slow time variation and external environmental uncertainties on MEMS-IMU, avoided speed measurement anomalies resulting from disturbance to inductive sensor, improved speed measurement & location accuracy and system stability, and performed test verification and analysis of engineering application.

Reference

- [1] GUO Xiao-zhou, WANG Ying, WANG Shi-xiong. Location and Speed Detection System for High-Speed Maglev Vehicle[J]. Chengdu: JOURNAL OF Southwest Jiao tong University. 2007.39(4).
- [2] JIANG Rui. The Study and Accomplishment of the Speed and Relative Location Detection Sensor for Low Speed Maglev Train[D]. Changsha: National University of Defense Technology Master thesis. 2010.
- [3] WANG Ying, LIAN Ji-san, Zhang Kun-lun. Speed measuring and locating system of maglev vehicle based on cross induction coils[J]. ELECTRIC DRIVE FOR LOCOMOTIVE, 2002, (02): 33-36+47.
- [4] XIONG Chun-hong, LI Xiaolong, HAN Jingru. Maglev Train Position Detection Based on Information Fusion of Particle Filter Algorithm[J]. Journal of East China Jiao tong University, 2015, 32(03): 12-15+113.

- [5] Jan Wendel, Oliver Meister, Christian Schlaile, Gert F. Trommer. An integrated GPS/MEMS-IMU navigation system for an autonomous helicopter[J]. Aerospace Science and Technology, 2006, 10(6).
- [6] BAO Chao, GUO Mei-feng, ZHOU Bin, LIU Gang. Miniaturization design of MIMU/GPS integrated navigation system[J]. Transducer and Microsystem Technologies, 2014, 33(01):116-119.
- [7] S. Nassar, K.P. Schwarz, A. Noureldin, N. El-Sheimy, Modeling inertial sensor errors using autoregressive (AR) models[C]. Proceedings of ION National Technical Meeting, Anaheim, 2003.
- [8] WU Yanpeng, YOU Zheng, REN Dahai. Unscented Kalman filter application in astronomical satellite attitude determination[J]. J Tsinghua Univ (Sci & Tech), 2003, Vol. 43, No. 8
- [9] Shin E H. Accuracy Improvement of Low Cost INS/GPS for Land Applications. Department of Geomatics Engineering University of Calgary Canada 2002.
- [10] JI Xun-sheng, WANG Shou-rong. Research on the MEMS Gyroscope Random Drift Error[J]. Journal of Astronautics, 2006, (04):640-642.
- [11] LI Jie, ZHANG Wen-dong, LIU Jun. Research on the Application of the Time-Serial Analysis Based Kalman Filter in MEMS Gyroscope Random Drift Compensation[J]. CHINESE JOURNAL OF SENSORS AND ACTUATORS, 2006, (05):2215-2219.
- [12] Mallat S, IEEE Trans. Pattern Analysis and Machine Intelligence, 1989, 11(7): 674.
- [13] ZHOU Yu-Feng, CHENG Jing-Quan. Wavelet transformation and its Applications[J]. PHYSICS 2008(1).
- [14] DONOHU, D. L., JOHNSTONE, I. M. Adapting to unknown smoothness via wavelet shrinkage. Journal of the American Statistical Association, 1995, 90(432): 1200-1224.
- [15] LI Q, TENG J F, WANG X, et al. Research of gyro signal denoising with stationary wavelets transform. Proceeding of IEEE Electrical and Computer Engineering. 2003.
- [16] Tang Wei, LI Shi-xin, LIU Lu-yuan, Yang Ye. Select of Wavelet Basis in Gyro Signal Processing[J]. Journal of Chinese inertial Technology 2002, (05):29-31.
- [17] Kok C W, Yoneyama K, Ikehara M. Symmetric Extension for Finite Length Multirate Signal Processing. Circuits and Systems, ISCAS. 2001.